

FULL PAPER

Humanoids Learn Touch Modalities Identification via Multi-Modal Robotic Skin and Robust Tactile Descriptors

Mohsen Kaboli*, Alex Long, and Gordon Cheng

*Institute for Cognitive Systems, Technical University of Munich, Germany**(08 Month 2015; acceted 09 Month 2015)*

In the paper, we present a novel approach for touch modality identification via tactile sensing on a humanoid. In this respect, we equipped a NAO humanoid with whole upper body coverage of multi-modal artificial skin. We propose a set of biologically inspired feature descriptors to provide robust and abstract tactile information for use in touch classification. These features are demonstrated to be invariant to location of contact and movement of the humanoid, as well as capable of processing single and multi-touch actions. To provide a comparison of our method, existing approaches were reimplemented and evaluated. The experimental results show that the humanoid can distinguish different single touch modalities with a recognition rate of 96.79% while using the proposed feature descriptors and SVM classifier. Furthermore, it can recognize multiple touch actions with 93.03% recognition rate.

Keywords: (tactile data processing, tactile feature descriptors, tactile learning, touch classification, artificial robotic skin, and humanoid robots)

1. Introduction

Recent advances in tactile sensing for robotics have opened up new pathways for humanoids to more accurately communicate with humans [1]. Through tactile interaction, various touch modalities may be carried out; a robot may be patted, slapped, punched, or tickled, with each action representative of a separate communicative intent. For any robotic system that is to work closely with humans, evaluation and classification of these touch modalities is vital. Humanoids should understand, just as humans do, that a slap is a form of negative feedback, that a pat is one of encouragement and so on [2]. To achieve this, combination of several layers of technology is required. A significant focus of the field has been on developing and extending tactile sensors utilized to collect and record tactile data. Less focus has been applied on the topic of processing and interpreting this data so as to provide meaningful and helpful information to the humanoid [3]. In this paper, we address the need for robust signal processing methods for tactile data.

As well as facilitating organic human-robot communication [4, 5], the classification and modeling of touch modalities has particular importance in applications such as disabled and aged care, nursing, and caring for patients with mild mental impairment, where a significant amount of communication is non-verbal. In particular, the use of both humanoid and non-humanoid robots have shown to significantly improve outcomes in remedial practice for children with autism [6]. Augmenting such robots with the ability to recognize and respond to social touch would further improve these outcomes.

*Corresponding author. Email: mohsen.kaboli@tum.de

2. BACKGROUND

2.1 *Tactile Sensing*

To date, many tactile sensors based on various sensing principles, e.g., resistive [7, 8], capacitive [9, 10], optical [11, 12] and piezoelectric [13, 14] etc., have been proposed [15]. However, in contrast to the rapid growth of the tactile sensor development, significantly less attention has been given to the research in processing and modeling of tactile data, such as in touch modality identification. Among many sensing methods suitable for touch modality recognition, in humanoid robots, artificial skins could be an appropriate choice. This is due to the high level of bio-mimicry they offer by providing sufficient resolution, distributed method to collect tactile data. While there is no well-accepted definition of what constitutes an artificial skin however, in general an artificial skin is a flexible, interlinked array of individual sensing elements capable of detecting external contact at a medium to high resolution [16]. Traditionally such skins are capable of detecting normal pressure/force, with more advanced skins possessing the capabilities to record shear force, acceleration, temperature and/or proximity. Kim *et al.* [17] developed such a skin using silicon micro-machining, allowing for the detection of normal and shear forces at high resolution. This skin was shown to be able to effectively measure normal force, hardness, slip, and touch. Such a sensor is ideal for touch classification since movements such as tapping and rubbing can be easily differentiated via the applied shear force. Restricting measurement to only force allows for a higher resolution, however it limits the ability to collect vibro-tactile data. RI-MAN [18] is one of the few humanoid robots capable interacting through whole-body contact, and is able to perform complex movements such as lifting a human with its arms. Semiconductor pressure sensors are placed in multiple sections of the robot body, providing tactile feedback on the position and orientation of the human subject. CB2 [19] is another example of full-body interaction, having a piezoelectric pressure sensitive layer embedded within its silicon covering. Here the goal was to develop a teaching by touching ability, where the robot learns basic movements through tactile interactions. Tajika *et al.* [20] developed a method for characterizing full-body human-robot haptic interaction via hierarchical clustering. Data was recorded from 256 piezoelectric tactile sensors embedded within a child-sized robots skin, and 27 haptic interactions, such as *shaking hands* and *holding up arm*, were accurately differentiated using unsupervised learning methods. Interactions were classified based on contact location and the manner of touching, however as only normal force data was collected, sliding movements were not considered, limiting the system. Iwata *et al.* [21] used the structural extension of self-organizing maps (SOMs) technique to classify touch modalities. A fur-based touch sensor used by Flagg *et al.* [22] to recognize three gestures. Gastaldo *et al.* [23] recently could discriminate paintbrush brushing, finger sliding, and washer rolling touch modalities from each other using a piezoelectric sensor arrays (PVDF). In [23], the authors offered a new pattern-recognition system, so called tensor-SVM and tensor-RLS in order to differentiate between rolling, sliding, and brushing.

2.2 *Existing touch classification approaches*

To the best of our knowledge there is only a few research that have addressed the problem of touch modality classification. There are three papers, in that they provide replicable, high-accuracy methodologies. In order to evaluate the effectiveness of the method presented in this paper, these methods which are summarised in table are adapted to our data, and evaluated in the paper [24–26]. The table 1 shows the summary of the existing touch classification approaches.

2.3 *Contribution*

The aim of the study is to augment a humanoid robot with the ability to recognize and classify various touch modalities. This is achieved through a multi-modal artificial skin covering large

Table 1. Summary of the existing approaches for touch modality identification

Study	Touch modalities	Sensing	Features	Learning Method
Silvera-Tawil [24]	Tap, Pat, Push, Stroke, Scratch, Slap, Pull, Squeeze	EIT force array	(1) Max intensity (2) Min intensity (3) Spatial resolution (4) Mean intensity (5) Contact time (6) Rate of change (7) Displacement (8) Location x and y (9) Max potential joint value (10) Min potential joint value	Logitboost
Koo [25]	Hit, Beat, Push, Rub	Low-resolution force array and accelerometer	(1) Total Force (2) Contact time (3) Contact area change	Decision tree
Naya [26]	Slap, Pat, Scratch, Stroke, Tickle	Ink-sheet force array	(1) Max total intensity (2) Max contact area (3) Temporal difference of total intensity at peak (4) Temporal difference of contact area at peak	K-NN and LDA

parts of a NAO humanoids upper body, as well as the use of novel biologically-inspired feature descriptors. These features improve on existing methods by providing;

- (1) *Multiple-touch action recognition*: Actions are able to be identified if enacted simultaneously with another action on a different body part.
- (2) *Dynamic cell selection*: Only those cells that are in contact during the action (as judged by proximity sensors) are considered in the feature space. This improves accuracy and reduces computational complexity, as well as allowing for the same classifier to run on
- (3) *Subject invariance*: Touch modalities carried out by previously unseen participants are still able to be accurately classified.
- (4) *Contact location invariance*: Accurate discrimination occurs regardless of the location or orientation of the interaction.
- (5) *Invariance to humanoid movement*: Consistent touch modality detection regardless of if the NAO is stationary or in motion.

We evaluated our method on a datasets of nine different touch modalities from twelve participants. Additionally, existing approaches utilizing similar methods we reimplemented and compared.

3. System Description

3.1 Multi-modal artificial skin

In order to emulate human sense of touch we have designed and manufactured the biologically inspired multi-modal and modular artificial skin called *Cellular Skin* [27]. Each skin cell has one local processor on the back side and one set of multi-modal tactile sensors on the front side, including one *three-axis accelerometer*; one *proximity sensor*; three *normal-force sensors*, and one *temperature sensor* (refer to Table 2). Skin cells together are directly connected via bendable and stretchable inter-connectors with each other. An unique cell ID is assigned to each skin cell within a network to efficiently handle a large number of skin cells. Additionally, the skin cells are placed in a 3D printed soft and silicone-based material to increase the contact area and friction properties and to improve the pleasant feeling (see Fig. 1).

3.2 Robot platform

The methods presented in this paper are independent of a specific humanoid robot. However, to validate our proposed methods we employed a small humanoid robot NAO from Aldebaran. NAO has 25 degrees of freedom is equipped with a 1.6 GHz Intel Atom Central Processing Unit, and its height and weight is 58 cm and 4.3 kg respectively.

3.3 Integrating skin on NAO

We covered the whole upper body of the NAO with 32 skin cells, 16 cells on the front and 16 cells on the back (see Fig. 1). All skin cells were connected by an interface board (converting all cell packets to standard UDP) to an Ethernet socket on the NAO's head. The cells transmit the obtained tactile information every 4 ms (250 Hz) to a data acquisition system integrated into NAO's PC for further processing. In this work NAO was in total equipped with 32 three-axis accelerometer sensors, 96 normal-force sensors, 32 proximity sensors, and 32 temperature sensors.

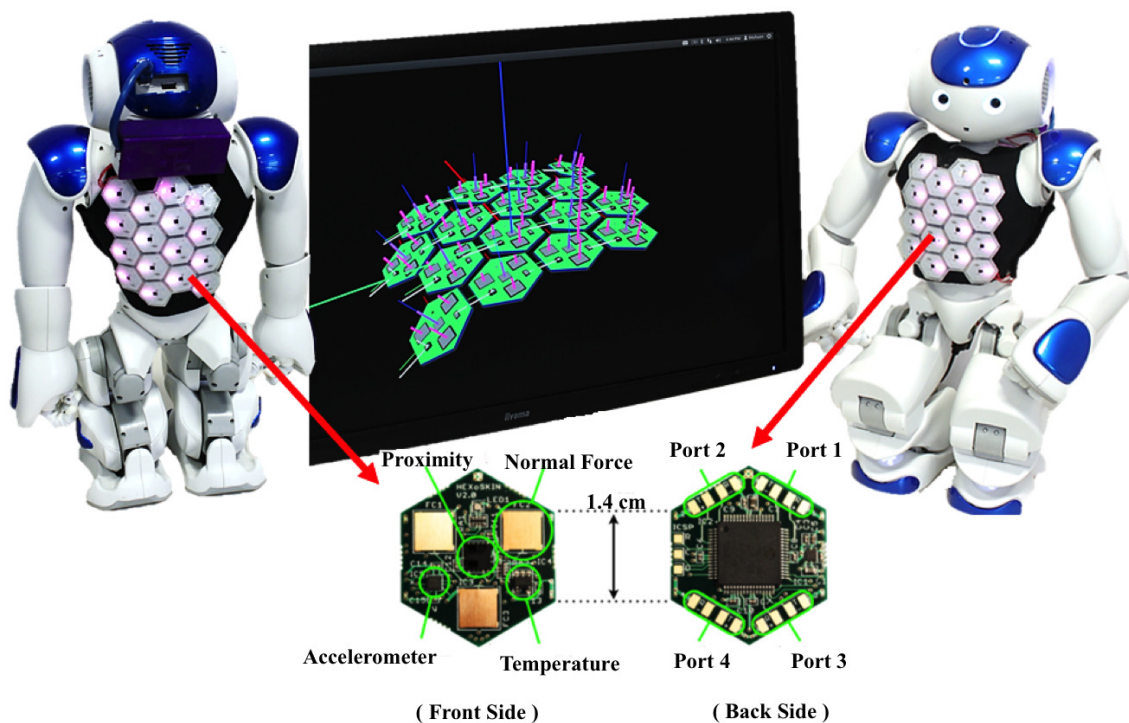


Figure 1. The upper body of the NAO was covered with 32 skin cells, 16 cells on the front and 16 cells on the back. The skin cells are called Cellular skin [27].

Table 2. Multi modal skin specifications.

Sensor	Acceleration	Force	Proximity (Pre-touch)	Temperature
Per Cell	1	3	1	1
Size in mm	$2.0 \times 2.0 \times 1.0$	$6.0 \times 6.0 \times 0.1$	$4.0 \times 4.0 \times 0.8$	$3.0 \times 3.0 \times 1.0$
Range	$\pm 2g$	$0 - 3N$	$1 - 200mm$	$-40^\circ C - 150^\circ C$
Resolution	$10bit$	$12bit$	$16bit$	$14bit$
Bandwidth	$0 - 1kHz$	$0 - 33kHz$	$0 - 250Hz$	$0 - 7Hz$

4. Touch Perception and Data Collection

4.1 Touch perception via multi-modal robotic skin

Tactile information corresponding to applied touch was measured via the multi-modal artificial skin on the front and back of the NAO. The generated vibration during touch presentation was measured by the existing three-axis accelerometer on each skin cell. The intensity of the applied touch was sensed by the normal force sensors. Pre-contact sensing was carried out via proximity sensors in each cell. The thermal sensors were used to sense the temperature of objects in contact with NAO's skin. The sensor readings corresponding to each cell-ID n_c are defined as

$\mathbf{A} = [\mathbf{a}_{n_a}^1, \mathbf{a}_{n_a}^2, \dots, \mathbf{a}_{n_a}^k, \dots, \mathbf{a}_{n_a}^{n_c}]$ for the *accelerometer*, where $\mathbf{a}_{n_a}^k \in \mathbb{R}^3$ denotes the measurements for each of the three accelerometer axes, $\mathbf{F} = [\mathbf{f}_{n_f}^1, \mathbf{f}_{n_f}^2, \dots, \mathbf{f}_{n_f}^k, \dots, \mathbf{f}_{n_f}^{n_c}]$ denotes the *normal-force* in which $\mathbf{f}_{n_f}^k \in \mathbb{R}^3$ represents the measurements of the three force sensors and $\mathbf{P} = [p^1, p^2, \dots, p^k, \dots, p^{n_c}]$ represents the output of the *proximity* sensors where $p^k \in \mathbb{R}$, and $\mathbf{T} = [t^1, t^2, \dots, t^k, \dots, t^{n_c}]$ denotes the *temperature* where $t^k \in \mathbb{R}$.

4.2 Data collection

Touch data collection was completed via 12 volunteers, with 6 females and 6 males. Each participant was given a description of the actions as described in Table 3. In order to allow for human-robot interactions to be as natural as possible no instructions were given to the subjects regarding the duration, orientation or location of contact. Each subject was free to complete the actions as he or she would do normally. Tactile data from two touch scenarios was collected for each participant namely *single touch* and *multiple touch*.

4.3 Single touch action

Single touch refers to a singular enactment of one of the touch modalities from Table 3 upon the surface of the NAO's skin (see Fig. 3). Humans can identify touch modalities invariant to the body motion. Therefore, single touch data were collected while the NAO was stationary, as well as when the NAO was in motion.

NAO in stationary position

For the stationary case, the NAO was in sitting position such that subjects had free access to front and back of the NAO.

- **Training data collection**

The training dataset was obtained from six of the twelve subjects, comprised of three males and three females. Each subject carried out each single-instance touch modality on the back of the NAO three times. Consequently, for each touch modality, 18 samples were collected (6 subjects \times 3 trials = 18 trials or a single touch modality), with 162 training samples in total (18 trials \times 9 touch modalities = 162).

- **Test data collection**

Humans can discriminate touch modalities regardless of the location of the received touch

on the body. Moreover, touch identification does not depend on the gender and age of the touch transmitter. Therefore, in this study, in order to assess the robustness of our proposed methods the unseen test data was collected from the remaining six subjects with different ages and nationalities. In addition, the test data was obtained from actions applied to the front of the NAO instead of the back. In this scenario, each touch modality was carried out four times. Subsequently, for each touch modality, 24 samples were collected (6 subjects \times 4 trials = 24 trials for a single touch modality), with 216 unseen test samples in total (24 trials \times 9 touch modalities = 216).

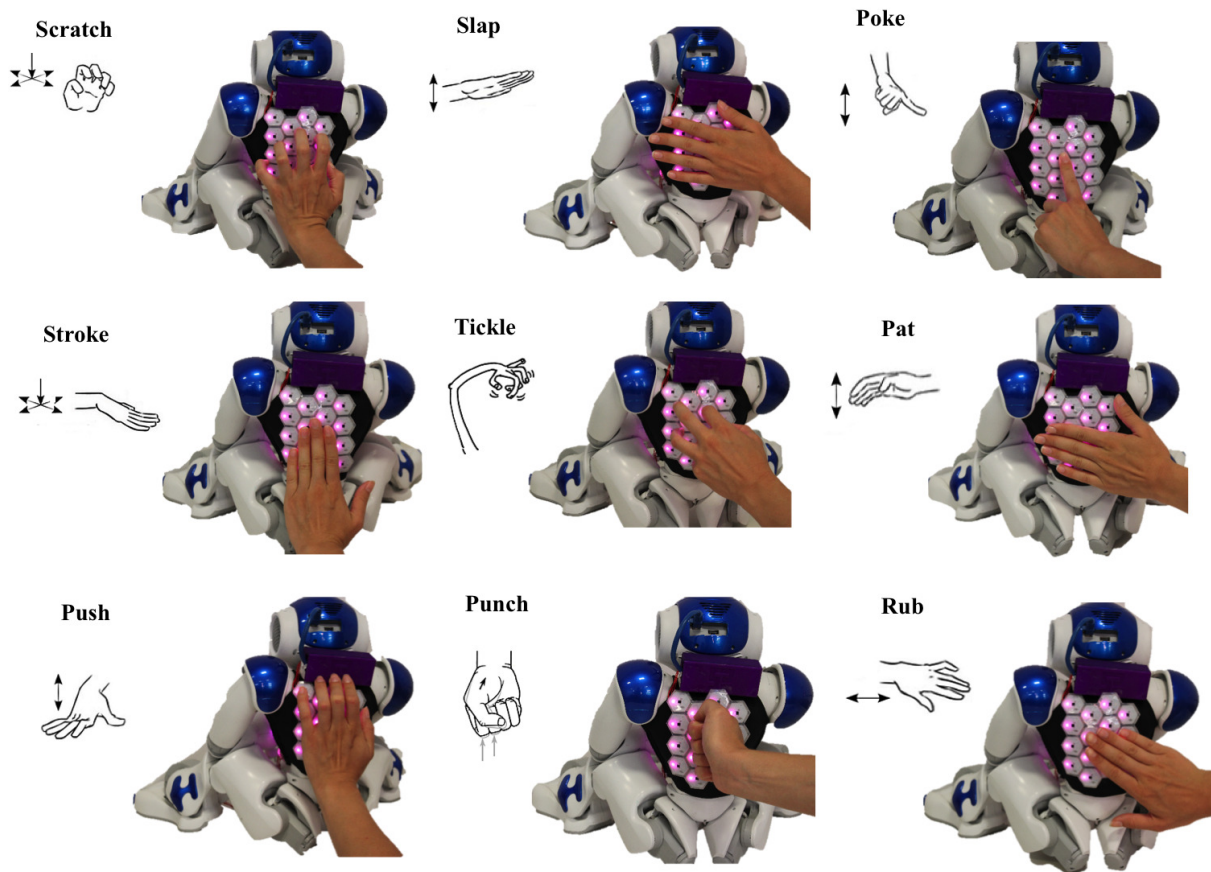


Figure 2. Illustrations of the nine touch modalities enacting on the NAO's body.

Table 3. Selected touch modalities.

Action	Description
Scratch	Contact with the fingertips or fingernails with movement tangential to the surface.
Tickle	Contact with the fingertips or fingernails with each finger moving independently and repeatedly along the skin.
Rub	Prolonged contact with the palm of the hand with movement tangential to the surface
Poke	Brief contact with the tips of one or more straightened fingers.
Stroke	Contact with the fingertips or upper sections of the finger moving simultaneously across the skin.
Punch	Brief contact applied by the base of a closed fist.
Pat	Two instances contact with the palm of the hand, relatively close together.
Push	Prolonged contact with the fingers or palm of the hand.
Slap	Brief contact with an open fist.

NAO in motion

In this scenario, NAO was in motion state. NAO was either walking toward and backward or sitting down and standing up continuously.

- **Training data collection**

Training touch samples were collected from six of the twelve subjects while NAO was continuously sitting down and standing up. Each subject was free to decide when to carry out the actions during the position transition. The rest of the procedure was the same as described for the training data collection in Sec. 4.3.

- **Test data collection**

In this scenario, whilst NAO was walking toward or backward the remaining six subjects performed the touch actions on the front of the NAO. Each subject could decide when to present the touch actions on front of the NAO during the motion or walking. The rest of the process was the same as explained in Sec. 4.3.

4.4 *Multiple simultaneous touch actions*

Multiple touch actions consist of two or more single actions performed simultaneously on different areas of the NAO. It is desirable for humanoid to possess the human ability to distinguish and identify simultaneously applied touch modalities. To evaluate this property, a subset of combinatory actions was selected from the possible combinations of the 9 individual actions. This subset was selected so as to provide a representative set containing at least one instance of each single-action, as well as focus on those actions likely to be performed together in natural communication. These actions are listed in Table 4. For the multiple touch case, data was collected while the NAO was moving. As was done in the single-touch case, the movement was a continual loop of sitting to standing up movements and vice versa. Each pair of single-actions was enacted simultaneously on the NAO in order to create their respective multiple touch action.

Table 4. Multiple touch actions.

Body Part		Combined Action								
Front	Poke	Tickle	Push	Slap	Rub	Stroke	Punch	Scratch	Pat	Slap
Back	Poke	Tickle	Rub	Push	Stroke	Stroke	Pat	Punch	Punch	Slap

- **Training data collection**

No training data was collected for the multiple touch case, as it is intended to be an evaluation dataset. The classifier used for evaluation was trained on the data previously collected in the single-touch case.

- **Test data collection**

A new group of six subjects not present in the previous single touch data collection, carried out the multiple touch actions on the NAO. Each action completed four times per subject (6 subjects \times 4 trials = 24 trials for each multiple touch modality). In total, this generated a dataset of 2 (front and back) \times 24 = 48 for each touch action.

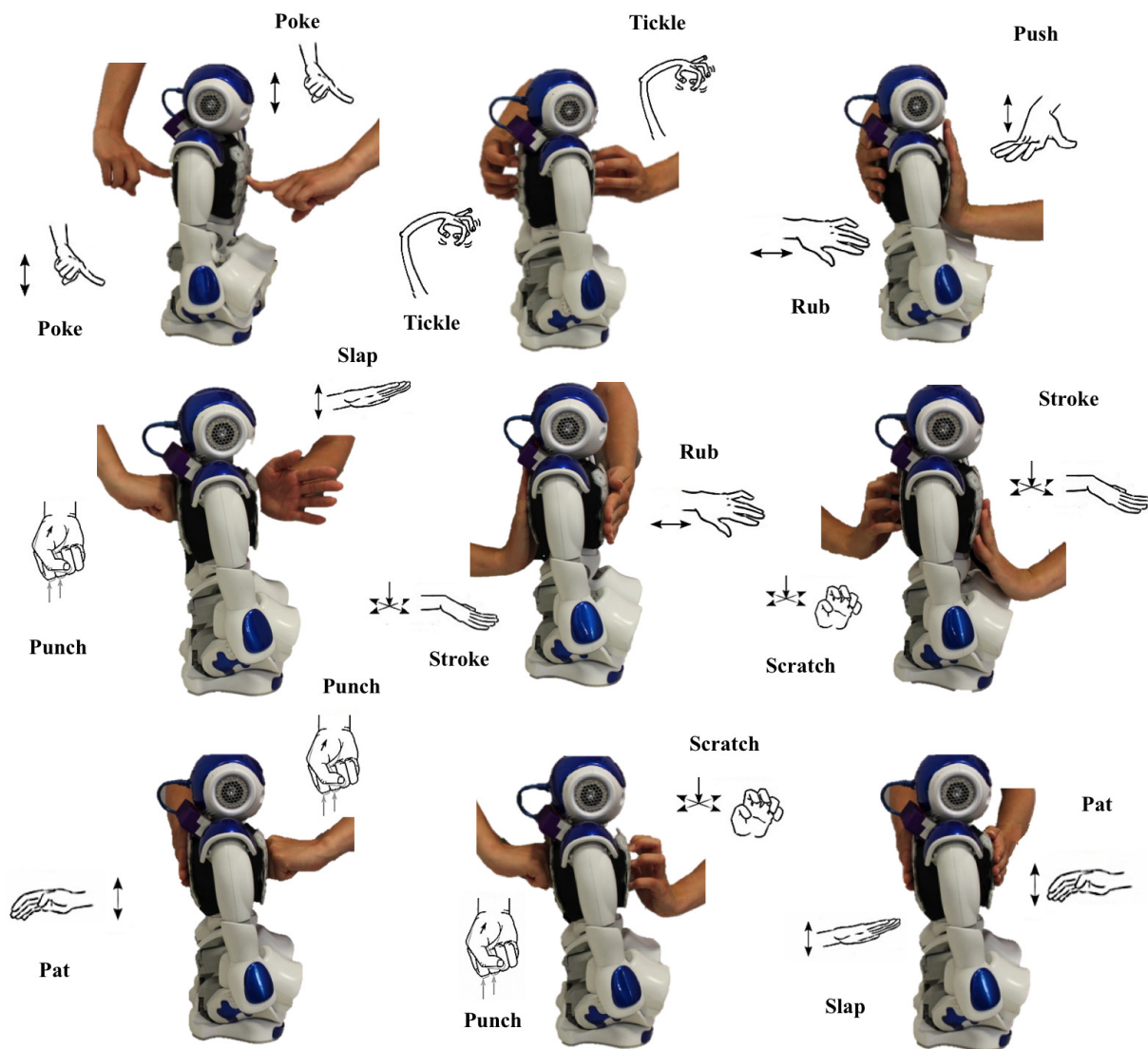


Figure 3. Illustrations of the multiple touch actions enacting simultaneously on the NAO's body.

5. Representative Of Touch Signals

5.1 Dynamic Cell Selection

The contact may occur at any arbitrary location along the NAO's skin during touch interaction. Therefore, NAO used the output of the proximity sensors existing on each skin cell to realize the location of a touch. In this experiment, all obtained proximity data were normalized to 0 and 1 (ζ_{n_c} in 1), i.e., the proximity output was equal to value 1 if a skin cell was in contact or in close contact ($d < 50 \text{ mm}$) with the subjects's hand, otherwise equal to 0 ($d > 50 \text{ mm}$).

$$\zeta_{n_c} = \begin{cases} 1 & \text{if } d < 50 \text{ mm} & \text{Contact} \\ 0 & \text{if } d > 50 \text{ mm} & \text{No - Contact} \end{cases} \quad (1)$$

where d is the distanced between hands of the subjects and NAO's skin and n_c is the assigned identification (ID) number of each cell. The output of the acceleration, normal force, and temperature sensors of the cells having proximity value equal to $\zeta_{n_c} = 1$ were considered for further

data processing. This decreases the computational cost of signal and information processing during the feature extraction and touch modeling by the NAO.

5.2 Pre-Processing

Before computing the feature descriptors, pre-processing of each tactile signal was required. In this respect the mean value of each obtained signal during a touch action was subtracted with the original raw signal (zero mean) to maximize useful information and minimize the effect of artifacts.

5.3 Proposed Feature Descriptors

In earlier works, researchers employed different signal processing techniques for interpreting touch information [24–26]. However, typically conventional methods deal with a large number of data points, thereby causing difficulties at the classification step. More features require more training samples which will result in increased computational complexity as well as the risk of over-fitting. To overcome these issues, we propose novel feature extraction techniques, inspired by the Hjorth parameters [28, 29]. Hjorth presented a set of parameters for real-time biological signal analyses (Electroencephalography). These parameters are called *Activity*, *Mobility*, and *Complexity*. The parameters represent the statistical properties of the signal in the time domain. Although these are defined in the time domain they can be interpreted in the frequency domain as well. The first parameter (2) is the total power of the signal. It is also the surface of the power spectrum in the frequency domain (Parseval's relation). The *Mobility* parameter, defined in (3), is determined as the square root of the ratio of the variance of the first derivative of the signal to that of the signal. This parameter is proportional to standard deviation of the power spectrum. It is an estimate of the mean frequency. The last parameter in (4) gives an estimate of the bandwidth of the signal, which indicates the similarity of the shape of the signal to a pure sine wave. Since the calculation of the Hjorth parameters is based on variance, the computational cost of this method is sufficiently low, which makes them appropriate descriptors for the real-time task.

$$Activity(x(t)) = Act(x(t)) = \frac{1}{N} \sum_{i=1}^N (x_i - \bar{x})^2 \quad (2)$$

$$Mobility(x(t)) = Mob(x(t)) = \sqrt{\frac{Activity\left(\frac{dx(t)}{dt}\right)}{Activity(x(t))}} \quad (3)$$

$$Complexity(x(t)) = Comp(x(t)) = \frac{mobility\left(\frac{dx(t)}{dt}\right)}{mobility(x(t))} \quad (4)$$

where $x(t)$ is the input signal and N is the number of the data sample.

The generated vibrations on the NAO's skin during touch execution were measured by the 3-axis accelerometer sensors. Since the three accelerometer components are highly correlated during the measurement, both linear correlation coefficient (5) and non-linear correlation coefficient (6) between each of the two axes of the accelerometer were considered as additional features.

$$Lcorr(x, y) = \frac{\sum_{i=1}^N (x_i - \bar{x})(y_i - \bar{y})}{\sqrt{\sum_{i=1}^N (x_i - \bar{x})^2} \sqrt{\sum_{i=1}^N (y_i - \bar{y})^2}} \quad (5)$$

$$Ncorr(x, y) = 1 - \frac{6 \sum_{i=1}^N (R_i)^2}{N(N^2 - 1)} \quad (6)$$

where R_i is the difference between the rank of x_i and the rank of y_i .

5.4 Final Feature Descriptors

Final feature descriptors of one skin cell

The tactile feature of one skin cell includes the linear and non-linear correlation coefficient between each two axes of accelerometer, namely $[Lcorr(a_x, a_y), Lcorr(a_x, a_z), Lcorr(a_y, a_z)]$ and $[Ncorr(a_x, a_y), Ncorr(a_x, a_z), Ncorr(a_y, a_z)]$ respectively. The feature also includes the Activity, Mobility, and Complexity parameter related to each of three acceleration signal component. The intensity of each touch action was measured via the force sensors. Therefore, the computed mean value of Activity corresponding to all three force sensors considered as an additional feature.

Final feature descriptors of a touch area

The tactile feature of a touch area with multiple skin cells can be defined with $[\mathbf{Lc}, \mathbf{Nc}, \mathbf{Ax}, \mathbf{Ay}, \mathbf{Az}, F]$ where

$$\mathbf{Lc} = \left[\frac{1}{N_c} \sum_{n_c=1}^{N_c} \zeta_{n_c} Lcorr(a_x^{n_c}(t), a_y^{n_c}(t)), \frac{1}{N_c} \sum_{n_c=1}^{N_c} \zeta_{n_c} Lcorr(a_x^{n_c}(t), a_z^{n_c}(t)), \frac{1}{N_c} \sum_{n_c=1}^{N_c} \zeta_{n_c} Lcorr(a_y^{n_c}(t), a_z^{n_c}(t)) \right] \quad (7)$$

$$\mathbf{Nc} = \left[\frac{1}{N_c} \sum_{n_c=1}^{N_c} \zeta_{n_c} Ncorr(a_x^{n_c}(t), a_y^{n_c}(t)), \frac{1}{N_c} \sum_{n_c=1}^{N_c} \zeta_{n_c} Ncorr(a_x^{n_c}(t), a_z^{n_c}(t)), \frac{1}{N_c} \sum_{n_c=1}^{N_c} \zeta_{n_c} Ncorr(a_y^{n_c}(t), a_z^{n_c}(t)) \right] \quad (8)$$

$$\mathbf{Ax} = \left[\frac{1}{N_c} \sum_{n_c=1}^{N_c} \zeta_{n_c} Act(a_x^{n_c}(t)), \frac{1}{N_c} \sum_{n_c=1}^{N_c} \zeta_{n_c} Mob(a_x^{n_c}(t)), \frac{1}{N_c} \sum_{n_c=1}^{N_c} \zeta_{n_c} Com(a_x^{n_c}(t)) \right] \quad (9)$$

$$\mathbf{Ay} = \left[\frac{1}{N_c} \sum_{n_c=1}^{N_c} \zeta_{n_c} Act(a_y^{n_c}(t)), \frac{1}{N_c} \sum_{n_c=1}^{N_c} \zeta_{n_c} Mob(a_y^{n_c}(t)), \frac{1}{N_c} \sum_{n_c=1}^{N_c} \zeta_{n_c} Com(a_y^{n_c}(t)) \right] \quad (10)$$

$$\mathbf{A}_z = \left[\frac{1}{N_c} \sum_{n_c=1}^{N_c} \zeta_{n_c} Act(a_z^{n_c}(t)), \frac{1}{N_c} \sum_{n_c=1}^{N_c} \zeta_{n_c} Mob(a_z^{n_c}(t)), \frac{1}{N_c} \sum_{n_c=1}^{N_c} \zeta_{n_c} Com(a_z^{n_c}(t)) \right] \quad (11)$$

$$F = \left[\frac{1}{N_c N_f} \sum_{n_c=1}^{N_c} \sum_{n_f=1}^{N_f} \zeta_{n_c} Act(F_{n_f}^{n_c}(t)) \right] \quad (12)$$

where N_c is the number of skin cells in a body part with multiple number of skin cells. N_f is the number of force sensors in one skin cell (in our case $N_f = 3$). Moreover, $\mathbf{A}_x \in \mathfrak{R}^3$, $\mathbf{A}_y \in \mathfrak{R}^3$, $\mathbf{A}_z \in \mathfrak{R}^3$, $\mathbf{Lc} \in \mathfrak{R}^3$, $\mathbf{Nc} \in \mathfrak{R}^3$, and $F \in \mathfrak{R}$. Therefore, the calculated final feature vector for each skin area has 16 data points instead of $\{ (\# \text{ skin cells}) \times [(\# \text{ of accelerometer axis}) \times (\# \text{ sampled data (250 Hz)})] + [(\# \text{ of force sensors}) \times (\# \text{ sampled data (1 KHz)})] \}$. By applying the proposed tactile feature descriptors on the measured tactile signals there is no need to reduce the dimensionality of data with further data processing (i.e. using Principal Component Analysis (PCA)).

6. Adapted existing touch classification approaches

In order to compare our proposed feature descriptors with the existing methods, we adapted the state-of-the-art feature descriptors so they could function on our data. This was because the data-set and experimental setup varies from paper to paper, and the exact methods cannot be directly reapplied. In some cases, features were discarded as they were not relevant for our data - such as detecting a repeating action when all touch modalities are single-instance. Those features that were re-implemented are listed below.

6.1 Adapted Naya [26]

- (1) *Max total intensity*: Max total force applied, calculated by finding the maximum of the total load datastream.

$$w_{peak} = \max \sum_{n_c=1}^{N_c} \sum_{n_f=1}^{N_f} F_{n_f}^{n_c}(t) \quad (13)$$

- (2) *Max contact area*: The contact area value obtained from the time of peak total load.

$$a_{peak} = \max \sum_{n_c=1}^{N_c} \sum_{n_f=1}^{N_f} b_{n_f}^{n_c}(t) \quad (14)$$

where

$$b_{n_f}^{n_c}(t) = \begin{cases} 1 & \text{for } F_{n_f}^{n_c}(t) \geq f_{thresh} \\ 0 & \text{otherwise} \end{cases} \quad (15)$$

- (3) *Temporal difference of total load*: Indicator of how sharp the peak for applied force is.

$$\delta_{w_{peak}} = \frac{\sum_{n_c n_f} |F_{n_f}^{n_c}(t_{max}) - F_{n_f}^{n_c}(t_{max} - 1)|}{\sum_{n_c n_f} F_{n_f}^{n_c}(t_{max})} \quad (16)$$

Where t_{max} is the time at which contact force was greatest.

- (4) *Temporal difference of contact area at total load*: Indicator of how sharply the contact area is changing at max force

$$\delta_{a_{peak}} = \frac{\sum_{n_c n_f} |b_{n_f}^{n_c}(t_{max}) - b_{n_f}^{n_c}(t_{max} - 1)|}{\sum_{n_c n_f} b_{n_f}^{n_c}(t_{max})} \quad (17)$$

6.2 Adapted Silvera-Tawil [24]

- (1) *Max Intensity*: Max value across all force sensors at any point in time during the action.
 (2) *Spatial resolution*: Ratio of elements containing at least 50% of the max intensity at the time of max intensity.

$$SR = \frac{1}{N_c N_f} \sum_{n_c=1}^{N_c} \sum_{n_f=1}^{N_f} c_{n_f}^{n_c}(t_{max}) \quad (18)$$

where

$$c_{n_f}^{n_c}(t) = \begin{cases} 1 & \text{for } F_{n_f}^{n_c}(t) \geq \frac{1}{2} w_{peak} \\ 0 & \text{otherwise} \end{cases} \quad (19)$$

- (3) *Mean of intensity*: Mean of the mean intensity across all sensors, across all time samples where action is observed.

$$MOI = \frac{1}{T N_c N_f} \sum_{t=0}^T \sum_{n_c=1}^{N_c} \sum_{n_f=1}^{N_f} F_{n_f}^{n_c}(t) \quad (20)$$

where T is the total number of time samples for the given action

- (4) *Contact Time*: Total time at least one force sensor is above threshold value, effectively measuring the duration of the action.
 (5) *Rate of intensity change*: Sum of the 2nd derivative of the absolute intensity change.

$$ROI = \sum_{n_c=1}^{N_c} \sum_{n_f=1}^{N_f} \frac{d^2 \left(|F_{n_f}^{n_c}(t) - F_{n_f}^{n_c}(t-1)| \right)}{dt^2} \quad (21)$$

6.3 Adapted Koo [25]

- (1) *Total Force*: Calculated using the variance of the accelerometer.

$$F_{total} = \text{var}(A_{rep}), \text{ where } A_{rep} \text{ is a representative accelerometer datastream} \quad (22)$$

- (2) *Contact Time*: Total time at least one force sensor is above threshold value, effectively measuring the duration of the action.
 (3) *Contact Area Change*: Sum of the changes in contact area

$$CAC = \sum_{n_c=1}^{N_c} \sum_{n_f=1}^{N_f} (b_{n_f}^{n_c}(t) - b_{n_f}^{n_c}(t-1)) \quad (23)$$

7. Experimental Results

7.1 Touch Modality Classification Results

The Support Vector Machine (SVM) [30] algorithms as a common supervised marginal learning approach and the linear kernel method were used to discriminate different touch. In order to find the optimal learning parameters for SVM, 5-fold cross validation (CV) was used. In this respect, the training data set was randomly split into 5 folds and during each evaluation, 4 of those were used for training and one was used for testing. This process was repeated 10 times to obtain an average performance on the evaluation sets. This entire process was repeated 20 times using different values for the leaning parameters to find the one with the lowest CV error. The SVM with optimal parameters was then re-trained with the entire training data set to obtain classification models. These classification models were used by NAO to predict the touch modalities for the unseen test data. The prediction results are reported in terms of recognition accuracy.

7.1.1 Single Touch Classification Results

Enacted Touch Location Invariance

As is possible for humans, humanoid robot also should be capable of identifying various touch modalities irrespective of the location in which they occur. To provide this capability with the NAO, the SVM along with the best learning parameters found via cross validation process was trained with the data obtained from *single-touch actions* enacted solely on the back of the NAO having the stationary position. Then the constructed touch classification models was used by the NAO to predict with the unseen test data set collected on the front of the NAO. In this scenario, NAO could classify 9 touch modalities with 96.79% recognition accuracy substantially higher than chance classifier. Table 5 shows the confusion matrix obtained from the classification procedure. The confusion matrix indicates how often a given touch action was misclassified as another one. Perfect classification would result in a diagonally-filled table. However, Table 5 shows that most errors involve touch modalities having similar action properties. For instance, Rub was confused with Stroke as they both have almost similar action properties. Moreover, Slap was identified as Pat and Punch since these touch modalities share almost identical action properties. However, the confusion matrix and the obtained results show that NAO was successfully able to discriminate different touch modalities regardless of the location of the enacted touch. Moreover, the achieved recognition results were independent on the subjects as the both training and unseen test data were collected with various subjects.

Enacted Touch Motion Invariance

NAO employed SVM with the linear kernel method to discriminate 9 different received touch actions. The optimal learning parameters were obtained from 5-fold cross validation, the detailed procedure of which has been explained above. The classifier was trained with the training data which was collected from the back of the NAO while it was moving. Then the constructed learning models were used to predict the unseen touch modalities in test data enacted on the front of the NAO while it was sitting down and standing up continuously. In this case, NAO achieved 94.4% classification accuracy. Regarding to the confusion matrix Table 6, Poke and Push were confused with each other as they have similar action properties. The confusion matrix also shows that Rub was misclassified as Push and Poke. These touch modalities are sharing similar actions properties compare to the others. Furthermore, in order to evaluate the robustness of our proposed approach the collected training data from the back of the NAO having stationary position was used to train the classifier. The constructed touch classification models then was evaluated by predicting with the unseen test data while NAO was moving. In this case, NAO could successfully discriminate 9 touch modalities through the actions properties with 92.52% recognition accuracy. The confusion matrix in Table 7 shows that push and Poke, Pat and Slap,

and Slap and Punch were confused two time with each other.

7.1.2 Multiple Touch Classification Results

Multiple touch classification was carried out by training SVM classifier on stationary, single-touch actions enacted on back side of the NAO. The multiple touch dataset of the 9 combinatory actions collected as an unseen test set. Each multiple touch was evaluated as the combination of two single actions. The relative position of each skin cell from its assigned ID, combined with the output of the proximity sensors, records and splits the combinatory actions into its constituent parts. Table 8 shows the obtained confusion matrix in which NAO achieved 93.03% multiple touch classification accuracy. Table 8 illustrates that poke, stroke, and Rub were confused with push. Moreover, Pat and Punch miss-classified two time with slap.

7.2 Touch Clustering Results

An important task for NAO was to qualitatively differentiate between varying categories of touch modalities. This means that touch actions having the same properties tend to be in the same cluster (unsupervised learning). In this respect, Expectation Maximization (EM) [31] algorithm was employed to categorize the selected touch actions. NAO employed the EM algorithm as an unsupervised learning approach to categorize enacted touch modalities through actions properties. The EM was trained with the entire unsupervised data set. A class to clustering approach was used to evaluate how well NAO can recognize the correct category of an unseen touch. In this approach, classes were assigned to the categories, based on the majority value of the class attribute within each categories. Later on, these assignments were used to compute the classification performance. shows the results of this experiment for the single touch and NAO with stationary position, single touch while NAO was moving, and multiple touch individually, in which our proposed feature descriptor used by NAO to extract informative data from the collected touch tactile data. From Fig .4 it is clear that NAO managed to recognize the categories of touch modalities with an accuracy significantly higher than chance. NAO could categorize single touch (stationary case) and single touch (while NAO was moving) with the accuracy of 81.83% and 78.91% respectively. Using the EM and similar learning procedure as above NAO also categorized the received single touch while EM was trained with the touch collected from NAO's back having stationary position and evaluated with the touch received on the front side while moving. The obtained unsupervised classification accuracy by the NAO was 77.55%. Moreover, using EM NAO could categorized the multiple touch successful with recognition rate of 80.10%.

7.3 Existing touch classification approaches comparison results

The touch feature descriptors proposed to discriminate 9 touch modalities by NAO were compared against the adapted state of the art touch identification methods. Each method was evaluated using the classifier utilized in the original paper, as well as with a standard SVM classifier. This was done as in some cases, in particular Koo, had features that functioned well with a specific type of learning method. Comparison with both a specified and standardized learning method provides greater insight into the role of the feature extraction. For comparison, the proposed features were evaluated on all listed classifiers, as well as the standard SVM. Each classifier was trained with the collected single touch action data set from the back of the NAO in which NAO had the stationary position. The constructed touch models then were evaluated by predicting with the unseen touch samples applied on front side of the NAO. The standardized SVM results placed the Hjorth-parameter based features with the highest accuracy, at 96.75% with the adapted Naya, Silvera-Tawil, and Koo features following with 67.3%, 56.2% and 53.6% respectively. The proposed features also demonstrated strong regularity across different learning methods. This strong regularity resulted in the proposed features outperforming other methods across the specified classifiers. Table 9 illustrates the results of the comparison between our

proposed touch discriminating methods and the state-of-the-art methods.

Table 5. Confusion matrix for single touch classification (NAO in stationary position).

	Pat	Poke	Punch	Push	Rub	Scratch	Slap	Stroke	Tickle
Pat	24	0	0	0	0	0	0	0	0
Poke	0	23	0	1	0	0	0	0	0
Punch	0	0	24	0	0	0	0	0	0
Push	0	0	0	24	0	0	0	0	0
Rub	0	0	0	0	22	0	0	2	0
Scratch	0	0	0	0	0	23	0	0	1
Slap	1	0	1	0	0	0	22	0	0
Stroke	0	0	0	0	0	0	0	24	0
Tickle	0	0	0	0	0	1	0	0	23

Table 6. Confusion matrix for single touch classification (NAO in motion).

	Pat	Poke	Punch	Push	Rub	Scratch	Slap	Stroke	Tickle
Pat	24	0	0	0	0	0	0	0	0
Poke	0	22	0	2	0	0	0	0	0
Punch	0	0	23	0	0	0	1	0	0
Push	0	2	0	22	0	0	0	0	0
Rub	0	1	0	1	22	0	0	0	0
Scratch	0	0	0	0	0	23	0	0	1
Slap	1	0	1	0	0	0	22	0	0
Stroke	0	1	0	1	0	0	0	22	0
Tickle	0	0	0	0	0	0	0	0	24

Table 7. Confusion matrix for single touch classification (Training: NAO in stationary position. Evaluation: NAO in motion).

	Pat	Poke	Punch	Push	Rub	Scratch	Slap	Stroke	Tickle
Pat	22	0	0	0	0	0	2	0	10
Poke	0	23	0	1	0	0	0	0	0
Punch	0	0	22	0	0	0	2	0	0
Push	0	0	0	22	0	0	0	2	0
Rub	0	0	0	0	22	0	0	2	0
Scratch	0	0	0	0	0	22	0	0	2
Slap	0	0	2	0	0	0	22	0	0
Stroke	0	0	0	2	0	0	0	22	0
Tickle	0	0	0	0	0	1	0	0	23

Table 8. Confusion matrix for multiple touch action classification (Training: NAO in stationary. Evaluation: NAO in motion).

	Pat	Poke	Punch	Push	Rub	Scratch	Slap	Stroke	Tickle
Pat	48	0	0	0	0	0	0	0	0
Poke	0	44	0	4	0	0	0	0	0
Punch	0	0	46	0	0	0	2	0	0
Push	0	2	0	44	0	0	0	2	0
Rub	0	0	0	2	44	0	0	2	0
Scratch	0	0	0	0	0	46	0	0	2
Slap	2	0	2	0	0	0	44	0	0
Stroke	0	0	0	4	0	0	0	44	0
Tickle	0	0	0	0	0	2	0	0	46

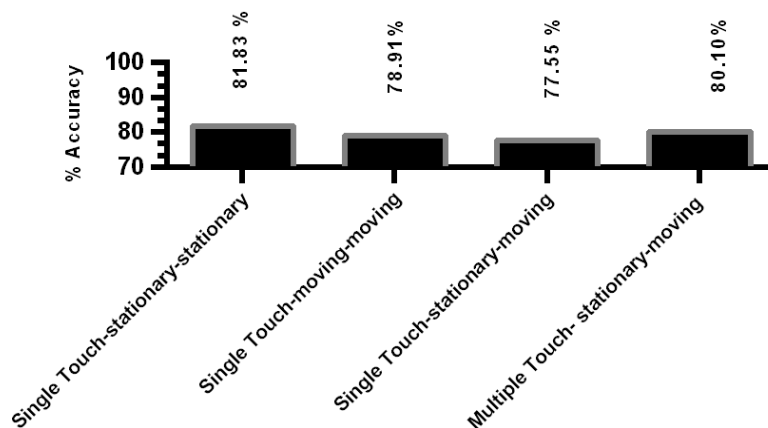


Figure 4. Single and multiple touch modality categorization results using EM and the proposed tactile descriptors. Single touch-stationary-stationary: EM was trained with unlabeled touch data from the back of the NAO (NAO was in stationary position) and evaluated with the test set obtained from the front of the NAO (NAO was in stationary position). Single touch-moving-moving: EM was trained and tested with touch data collected from back and front of the NAO respectively (in both case NAO was in motion). Single touch-stationary-moving: EM was trained and tested with touch data collected from back (NAO was in stationary position) and front of the NAO respectively (NAO was in motion). Multiple touch-stationary-moving: EM was trained with single touch data collected from the back of the NAO (NAO was in stationary position) and evaluated with multiple touch actions from front of the NAO (NAO was in motion)

Table 9. Comparison with the adapted existing touch classification approaches

Study	Features	Classifier (% correctly classified)			
		K-NN	Decision Tree	Logitboost	SVM
Adapted Naya	(1) Max total intensity (2) Max contact area (3) Temporal difference of total intensity at peak (4) Temporal difference of contact area at peak	60.4 %	—	—	67.3%
Adapted Silvera	(1) Max intensity (2) Spatial resolution (3) Mean intensity (4) Contact time (5) Rate of change	—	—	59.4%	56.2%
Adapted Koo	(1) Total Force (2) Contact time (3) Contact area change	—	58.1%	—	53.6%
Our Proposed Features	(1) Activity (2) Mobilty (3) Complexity (4) Linear Correlation (5) Non-linear Correlation	95.1 %	96.8 %	94.4%	96.75%

8. Discussion

This paper addressed the problem of humanoid touch modality classification through the use of multi-modal tactile sensing and novel feature descriptors. The results obtained from several experimental setups demonstrate the robustness of the feature descriptors. In the single action stationary case, the NAO was trained with actions applied to it's back side and tested on actions performed on the front. The resultant high recognition rate shows the invariance of the features to the location of contact. This was extended in the multiple-touch case where actions were performed simultaneously to one another on alternate sides of the NAO. These actions comprised a test set which was evaluated on a classifier trained exclusively on the data from single touch case. The high level of discrimination demonstrates the ability for the humanoid to recognize both single and multi-touch actions. Evaluating on a test set comprised of subjects the NAO had not previously interacted with resulted in high classification accuracy illustrates invariance to the particular person performing the action. Finally, testing on data collected which the NAO was in motion, showed that performance was not effected. To compare our method with the existing approaches, those that addressed the problem of touch modality classification were adapted to be compatible with our system. The comparison results show that our system, across multiple learning methods, for single touch classification, substantially outperforms the adapted approaches. Existing approaches, such as Koo and Silvera-Tawil, commonly use a high spatial resolution sensor. The artificial skin used in our method, however, has a comparatively low spatial resolution. This reduction in tactile information should result in a decreased classification accuracy, however this was compensated by the proposed feature descriptors. This is due to the features extracting key information from the raw signals without requiring further dimensionally reduction or feature selection. A significant advantage to the features is the built-in dynamic cell selection. By thresholding the proximity data to detect contact, only those cells being directly interacted with contribute towards the feature vector. The key result of this inclusion is the decrease in computational cost, as only those datastreams directly associated with the action are processed. This is especially significant when large amount of cells are used, such as if a full-size humanoid was to be covered. Furthermore, because only the in-contact cells are included in the features, actions of differing duration can be directly compared. Finally, the proximity thresholding also makes it trivial to differentiate between periods of contact and no-contact, simply by examining if any cells are being interacted with or not.

9. Conclusion

In this paper we address the need for robust processing of tactile data for touch modality classification. Physical interaction is an important part of natural communication, and humanoids must be able to deal with such contact both accurately and robustly. In this paper we have introduced novel biologically inspired feature descriptors that require no further reduction in data through methods such as PCA or LDA. These features were shown to function in a highly robust way, with high accuracy being obtained while introducing movement, changing the person completing the actions, and allowing free selection of location and orientation. Multi-touch actions were also completed and shown to be understood and identified with a similarly high level of accuracy. There are several avenues through which the system can be extended. Most obvious is the mapping of actions to behavior, such as to register negative feedback when slapped, or to move away when pushed. Human and non-human contact can also be implemented by leveraging the temperature sensors present in the skin. By detecting a raise in temperature, the system could identify human contact, however there are difficulties this would be constrained in scope to scenarios where there is a noticeable difference between the human temperature and the surrounding environment. Covering the whole body of the humanoid with artificial skin can be considered as a future work in which there will be some crucial challenges to tackle such as tactile signal reading and processing from whole body skin. Especially when a humanoid robot will be in contact with humans and objects at the same time. The potential solution for such a challenge is the integration of the proposed features descriptors and the event based tactile processing. This approach can also be used to optimize the amount of information within the distributed network of the sensors.

Acknowledgment

This work is supported by the European Commission under grant agreements PITN-GA-2012-317488-CONTEST. Many thanks to Dr. Jun Nakanishi for the proof reading and his useful comments.

References

- [1] B. D. Argall, and A.G Billard. A survey of Tactile HumanRobot Interactions. *Robotics and Autonomous Systems*, 58: 1159-1176, 2010.
- [2] A. L. Thomaz, G. Hoffman, and C. Breazeal. Reinforcement Learning with Human Teachers: Understanding How People Want to Teach Robots. *IEEE International Symposium on Robot and Human Interactive Communication*, pages 352-357, 2006.
- [3] R. S. Dahiya, G. Metta, Giorgio, M. Valle, and G. Sandini. Tactile sensing from humans to humanoids. *IEEE Transaction on Robotics*, 26:1-20, 2010.
- [4] R. S. Dahiya, and M. Valle. *Robotic Tactile Sensing*. Springer, ISBN 978-94-007, 2013.
- [5] A. Silvera-Tawil, D. Rye, and M. Velonaki. Artificial skin and tactile sensing for socially interactive robots: A review. *Robotics and Autonomous Systems*, 63:230-243, 2015.
- [6] H. Kozima, C. Nakagawa, and Y. Yasuda. Interactive robots for communication-care: A case-study in autism therapy. *IEEE International Workshop on Robots and Human Interactive Communication*, pages 341-346, 2005.
- [7] M. Kaltenbrunner, T. Sekitani, J. Reeder, T. Yokota, K. Kuribara, T. Tokuhara, M. Drack, R. Schwödiauer, I. Graz, S. Bauer-Gogonea, S. Bauer, Siegfried and T. Someya. An ultra-lightweight design for imperceptible plastic electronics. *Nature*, 499:458-63, 2013.
- [8] M. W. Strohmayer, H. Worn, and G. Hirzinger. The DLR Artificial Skin Part I: Uniting Sensitivity and Robustness. *IEEE International Conference on Robotics and Automation*, pages 1012-1018, 2013.
- [9] A. Schmitz, P. Maiolino, M. Maggiali, L. Natale, G. Cannata, Giorgio, and G. Metta. *Methods*

- and technologies for the implementation of large-scale robot tactile sensors. *IEEE Transactions on Robotics*, 27:389-400, 2011.
- [10] J. Ulmen, and M. Cutkosky. A Robust, Low-Cost and Low-Noise Artificial Skin for Human-Friendly Robots. *IEEE International Conference on Robotics and Automation*, pages 4836-4841, 2010.
 - [11] Y. Ohmura, Y. Kuniyoshi, and A. Nagakubo. Conformable and Scalable Tactile Sensor Skin for Curved Surfaces. *IEEE International Conference on Robotics and Automation*, Pages 1348-1353, 2006.
 - [12] H. Xie, H. Liu, S. Luo, L. D. Seneviratne, and K. Althoefer. Fiber optics tactile array probe for tissue palpation during minimally invasive surgery. *IEEE*, pages 2539-2544, 2013.
 - [13] R. S. Dahiya, G. Metta, M. Valle, A. Adami, and L. Lorenzelli. Piezoelectric oxide semiconductor field effect transistor touch sensing devices. *Applied Physics Letter*, pages 2-4, 95:2009
 - [14] T. V. Papakostas, J. Lima, and M. Lowe. A Large Area Force Sensor for Smart Skin Applications. *IEEE Sensors*, 2:1620-1624, 2002.
 - [15] P. Puangmali, K. Althoefer, L. D. Seneviratne, and D. Murphy, and P. Dasgupta. State-of-the-art in force and tactile sensing for minimally invasive surgery *IEEE Sensor*, 8:371-380, 2008.
 - [16] A. Lucarotti, C. M. Oddo, N. Vitiello, and M. C. Carrozza. Synthetic and bio-artificial tactile sensing: A review. *IEEE Sensors*, 13:1435-1466, 2013.
 - [17] K. Kim, K. R. Lee, D. S. Lee, N. K. Cho, W. H. Kim, K. B. Park, H. D. Park, Y. K. Kim, Y. K. Park, and J. H. Kim, Jong-Ho. A silicon-based flexible tactile sensor for ubiquitous robot companion applications. *Journal of Physics: Conference Series*, 34:399-403, 2006.
 - [18] T. Mukai, S. Hirano, and Y. Kato. Fast and accurate tactile sensor system for a human-interactive robot. *INTECH Open Access Publisher*, 2008.
 - [19] T. Minato, Y. Yoshikawa, T. Noda, S. Ikemoto, H. Ishiguro, and M. Asada. A child robot with biomimetic body for cognitive developmental robotics. *IEEE-RAS International Conference of Humanoid Robot*, pages 557-562, 2008.
 - [20] T. Tajika, T. Miyashita, H. Ishiguro, and N. Hagita. Automatic categorization of haptic interactions -what are the typical haptic interactions between a human and a robot? *IEEE International Conference on Humanoid Robots*. pages 490-496, 2006.
 - [21] A. Iwata, and S. Sugano. Human-robot-contact-state identification based on tactile recognition. *IEEE Transaction on Industrial Electronics*, 52:1468-1477, 2005.
 - [22] A. Flagg, D. Tam, K. MacLean, and R. Flagg. Conductive fur sensing for a gesture-aware furry robot. *IEEE Haptics Symposium (HAPTICS)*, pages 99104, 2012.
 - [23] P. Gastaldo, L. Pinna, L. Seminara, and M. Valle, and R. Zunino. A tensor-based approach to touch modality classification by using machine learning. *Robotics and Autonomous Systems*, 63:268-278, 2015.
 - [24] A. S. Tawil, V. Rye, M. Velonaki. Interpretation of the modality of touch on an artificial arm covered with an EIT-based sensitive skin. *The International Journal of Robotics Research*, 31:1627-1641, 2012.
 - [25] S. Y. Koo, J. G. Lim, and D. S. Kwondoi. Online touch behavior recognition of hard-cover robot using temporal decision tree classifier. *IEEE International Symposium on Robot and Human Interactive Communication*, Pages 425429, 2008.
 - [26] A. Naya, J. Yamato, and K. Shinozawa. Recognizing Human Touching Behaviors using a Haptic Interface for a Pet-robot Touching behaviors and experiment. *IEEE International Conference on Systems, Man, and Cybernetics*. pages 3-7, 1999.
 - [27] P. Mittendorfer, and G. Cheng. Humanoid Multimodal Tactile-Sensing Modules. *IEEE Transactions on Robotics*, 27:401-410, 2011.
 - [28] Bo, Hjorth. EEG analysis based on time domain properties. *Electroencephalography and clinical neurophysiology*, 29:306-310, 1970.
 - [29] M. Kaboli, P. Mittendorfer, V. Hugel, and G. Cheng. Humanoids learn object properties from robust tactile feature descriptors via multi-modal artificial skin. *IEEE International Conference on Humanoid Robots*, pages 187-192, 2014.
 - [30] C. Cortes, and V. Vapnik. Support-vector networks. *Journal in Machine learning*, 20:273-297, 1995.
 - [31] A. P. Dempster, N. M. Laird, and D. B. Rubin. Maximum likelihood from incomplete data via the EM algorithm. *Journal of the Royal Statistical Society*, 39:1-38, 1977.

Biographies:



Mohsen Kaboli received his Bachelor in Electrical and Electronic Engineering and Master in Wireless Systems and Signal Processing from the Royal Institute of Technology (KTH University) in Stockholm, Sweden, in 2011. He joined Idiap lab/EPFL university as a research assistant in March 2011. Since April 2013, he has been with the Tactile Sensing Group with Prof. Gordon Cheng, Institute for Cognitive Systems, Technische Universität München in Munich, Germany. His current research interests include Tactile Learning and Tactile Transfer Learning in Robotic Systems.



Alex Long was born 1992. He completed his Bachelor of Engineering from the University of Queensland majoring in electrical engineering. He is currently enrolled in a double-masters program with the Technische Universität München, Munich, Germany and the University of Queensland, to be completed in 2015. His current research interests include humanoid robotics, cognitive systems, and reinforcement learning.



Gordon Cheng is the Professor and Chair of Cognitive Systems, and founding Director of the Institute for Cognitive Systems, Technische Universität München, Munich, Germany. He was the Head of the Department of Humanoid Robotics and Computational Neuroscience, ATR Computational Neuroscience Laboratories, Kyoto, Japan, from 2002 to 2008. He was the Group Leader for the JST International Cooperative Research Project, Computational Brain, from 2004 to 2008. He was designated a Project Leader from 2007 to 2008 for the National Institute of Information and Communications Technology of Japan. He has held visiting professorships worldwide in multidisciplinary fields comprising mechatronics in France, neuroengineering in Brazil, and computer science in the USA. He held fellowships from the Center of Excellence

and the Science and Technology Agency of Japan. Both of these fellowships were taken at the Humanoid Interaction Laboratory, Intelligent Systems Division at the Electrotechnical Laboratory, Japan. He received the Ph.D. degree in systems engineering from the Department of Systems Engineering, The Australian National University, in 2001, and the bachelors and masters degrees in computer science from the University of Wollongong, Wollongong, Australia, in 1991 and 1993, respectively. He was the Managing Director of the company G.T.I. Computing in Australia. His current research interests include humanoid robotics, cognitive systems, brain machine interfaces, biomimetic of human vision, human-robot interaction, active vision, and mobile robot navigation. He is the co-inventor of approximately 15 patents and has co-authored approximately 180 technical publications, proceedings, editorials, and book chapters.